Electronic Supplementary Material (ESI) for Chemical Communication.
This journal is © The Royal Society of Chemistry 2022

Electronic Supplementary information

A bipolar porphyrin molecular for stable dual-ion symmetric batteries with high potential

Youlian Zeng, Jiarong Zhou, Jiahao Zhang, Yao Liao, Caihong Sun, Yachao Su, Ping Gao* and Songting Tan*

Key Laboratory of Environmentally Friendly Chemistry and Application of Ministry of Education, College of Chemistry, Xiangtan University, Xiangtan 411105, P. R. China.

*E-mail: ping.gao@xtu.edu.cn(P. Gao), tanst2008@163.com (S. Tan)

1. Materials, characterization and synthesis

1.1 Materials and characterization

Polyvinylidene fluoride (PVDF), acetylene black, N-methyl-2-pyrrolidone (NMP), and stainless steel (316L, 12 mm in diameter, thickness about 15 μm) and Glass microfiber filters (Whatman, GF/D) were purchased commercially. All solvents and reagents were purchased from Chemical Great Wall and Energy Chemical company, which were used as received without further purification. The crystal structure of material was characterized by XRD (Model D8-Advance, Germany) using the Cu Kα radiation (λ= 1.5418 Å) at 40 mA and 40 kV. The particle morphology was studied using field emission scanning electron microscope (FESEM, Hitachi S-4800). The attenuated total reflectance-fourier transformation infrared (ATR-FTIR) spectrum was obtained on a Thermo Fisher Nicolet IS50 ATR-FTIR spectrometer from 600 cm^{-1} to 4000 cm^{-1}. XPS was recorded on an Escalab250Xi (Thermo Scientific), using monochromatized Al Kα radiation (1486 eV). The pass energy for survey spectra was 100 eV, for detail spectra the energy was 30 eV. The binding energies of all spectra were calibrated concerning the C1s peak of ubiquitous carbon at a binding energy of 284.7 eV. ^1H NMR spectra were recorded with a Bruker Avance 400 instrument. Mass spectrometry (MS) was performed on a Bruker Aupoflflex III MALDI-TOF Analyzer using CCA as the matrix. Cv and electrochemical impedance using electrochemical workstation (DH7000C, Jiangsu Donghua Analysis Instruments Co. Ltd.)

1.2 Synthesis

The synthetic procedure of compound 1 and TP molecular is shown in Scheme S1.

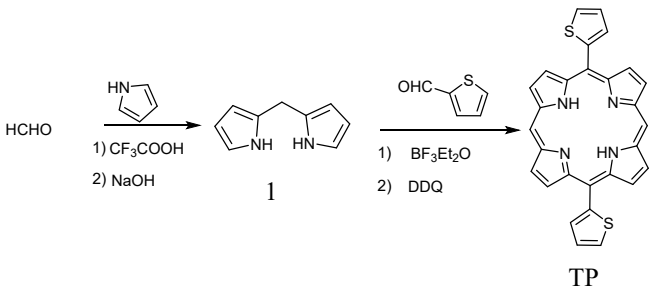

Scheme S1. Synthetic procedures of TP molecular.

1.2.1 Synthesis of compound 1

Pyrrole (17 mL, 0.25 mol) was degassed by Ar for 15 min. Then formalin (3 mL, 0.05 mol) was added under Ar atmosphere. After the mixture was cooled down to 0°C, 0.1 mL CF_3COOH was added. The reaction was stirred for 30 min. Then sodium hydroxide solution was added, and the reaction was stopped. The organic and aqueous phases were separated by extraction with dichloromethane and distilled water. The obtained organic phase was subjected to column

chromatography (petroleum ether: dichloromethane = 3:1) to obtain the compound 1 as white crystals (1.5g yield: 20%).

1.2.2 Synthesis of 5,15-di(thiophen-2-yl) porphyrin (**TP**)

Compound 1 (1.5 g, 10 mmol) and thiophene-2-carbaldehyde (0.84 g, 15 mmol) were added to 700 mL DCM, and this mixture was degassed with Ar at 0 ^{o}C. Boron trifluoride ether solution (0.1 mL) was added, and the reaction was stirred for 30 min. Then 2,3-dichloro-5,6-dicyano-1,4-benzoquinone (DDQ) (3.390 g, 15 mmol) was added, and the reaction was stirred for 30 min. After the reaction was completed, the product was subjected to column chromatography (dichloromethane as solvent) and then the solvent was removed by distillation under reduced pressure to obtain a crude product, which was then precipitated with dichloromethane and methanol by suction filtration to obtain purple crystals (400 mg, yield: 11.2%). ^{1}H NMR (400 MHz, chloroform-d) δ: 10.30 (s, 2H), 9.39 (s, 4H), 9.29 (s, 4H), 7.96 (s, 2H), 7.90 (s, 2H), 7.55 (s, 2H), -3.00 (s, 2H).

2. Assembly of cells

2.1 Assembly of half cells

For Li-ion half cells, the electrolytes were 1M $LiPF_6$ in PC. Lithium foil was used as a counter electrode. The potential of 1.8-4.5V (Vs. Li^+/Li) and 0.01-3.0V (Vs. Li^+/Li) were used for the study of TP as a cathode and an anode, respectively.

2.2 Assembly of all-organic symmetric cells

For Li-ion all-organic symmetric cells, TP was employed as both anode and cathode. Both the TP cathode and the TP anode was initially active by using galvanostatic charge and discharge, making cathode keep full charged state and anode remain full discharged state. The mass of active material in the anode is the twice that of the cathode. The active material mass loading of positive electrodes was about 0.61 -1.06 mg cm^{-2}. The active material mass loading of negative electrodes was about 1.06 -1.5 mg cm^{-2}.

2.3 Electrochemical measurements

All the electrochemical performance of the cell was performed by using CR2032 coin-type cells in an Ar-filled glove box. The TP electrodes were prepared by mixing TP, acetylene black and polyvinylidene fluoride (PVDF) with a weight ratio of 5:4:1 to form a slurry, then the slurry was coated onto 316L stainless steel current collector and dried at 110 ℃ for 24 h. And the acetylene black electrode was prepared by mixing acetylene black, PVDF with a weight ratio of 9:1. The TP electrode which test on an optical spectrogram was prepared by mixing 80 wt%TP, 10 wt % acetylene black, and 10 wt% polyvinylidene fluoride (PVDF). The active material mass loading of

all electrodes was about 0.73 -1.5 mg cm^{-2}.

3. Supplementary Figures

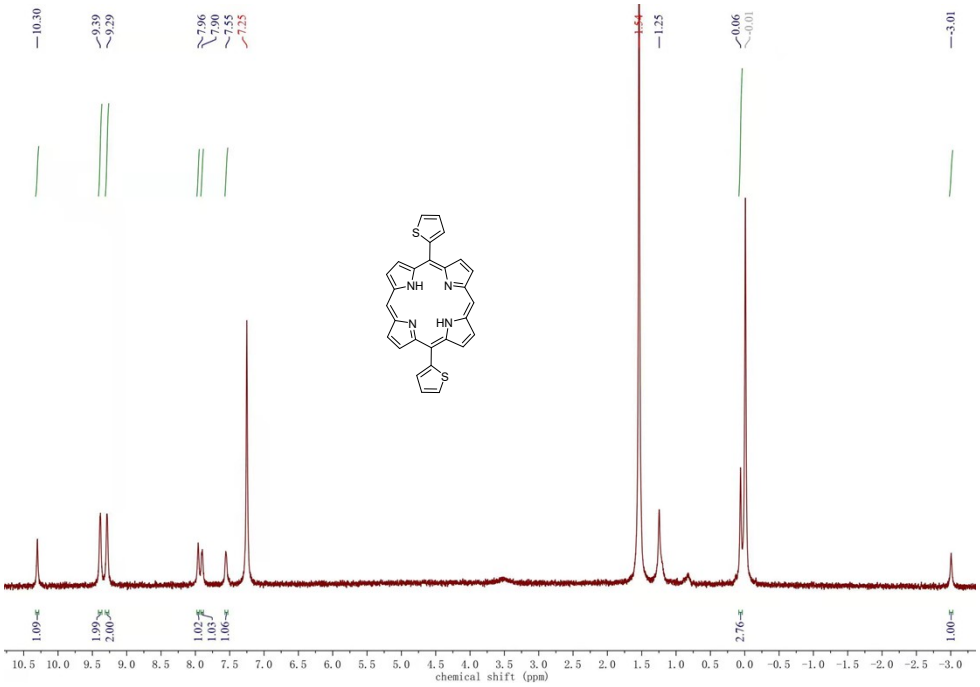

Fig. S1. [1]HNMR spectra of TP**.**

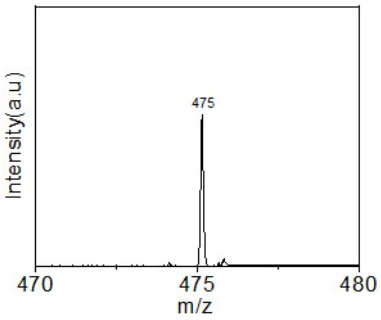

Fig. S2. Mass spectra of TP.

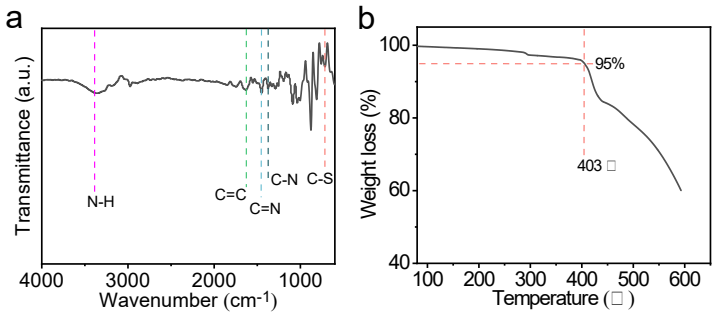

Fig. S3. (a) The FTIR spectra and (b) TG curve of TP.

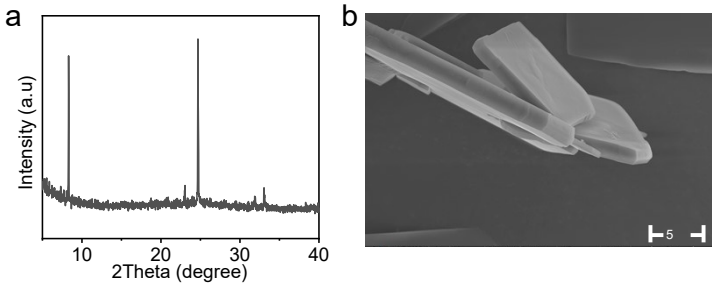

Fig. S4. (a) XRD pattern and (b) scanning electron microscopy image of TP.

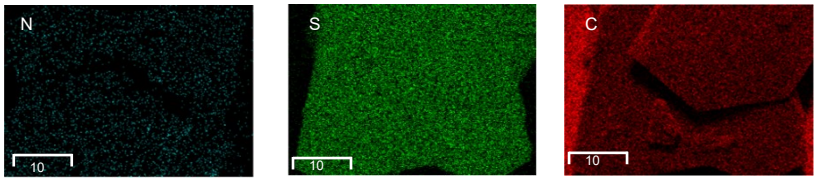

Fig. S5. Element mapping image of N, S and C.

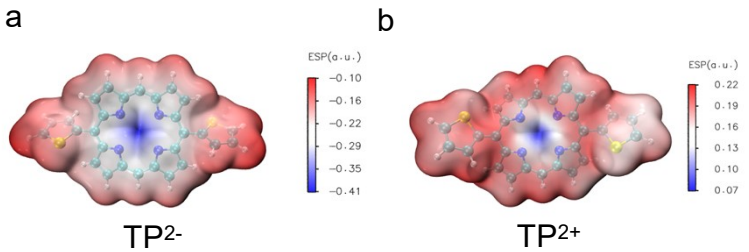

Fig. S6. a) Reduction state and b) oxidation state of TP.

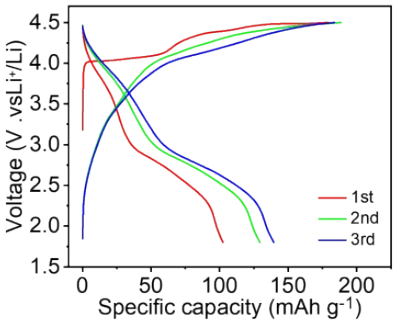

Fig. S7. Charge - discharge curves of TP cathode.

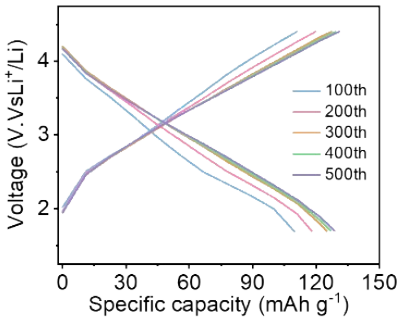

Fig. S8. Charging and discharging curves of the TP cathode in the 100th, 200th, 300th, 400th, 500th cycles.

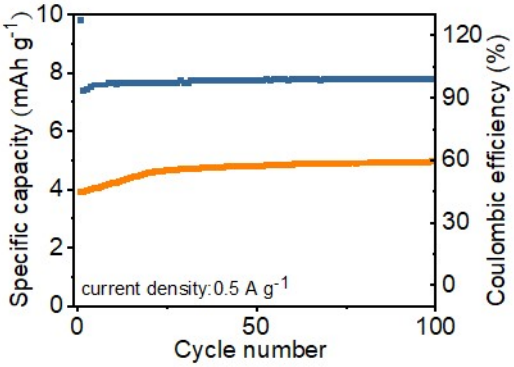

Fig. S9. The capacity contribution of acetylene back when it was used as the cathode.

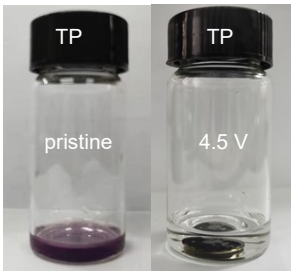

Fig. S10. Image of pristine and charged to 4.5 V electrodes which were soaked in PC solvent for 72 hours.

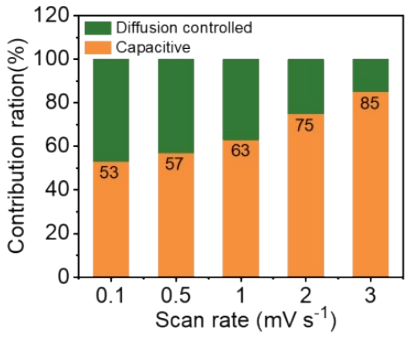

Fig. S11. The capacitive contribution at different scan rate.

To study the charge storage performance of TP as an anode, a voltage window of 0.01–3.0 V was used. At current densities of 0.1, 0.3, 0.5, 1, and 2 A g^{-1}, the TP electrode delivered discharge rial, which can be ascribed to the insertion of both Li^+ and PF_6^- ions into the cathode region, while only Li+ cations interacted in the anode region. Meanwhile, this result further confirmed capacities of 200, 144, 130, 108, and 87 mAh g^{-1}, respectively. When the current density was returned to 0.1 A g^{-1}, the capacity recovered to 185 mAh g^{-1} (Fig. S12b, ESI†), indicative of excellent rate performance. The TP anode displayed a high reversible capacity of 121 mAh g^{-1} (the acetylene black contributed a reversible capacity of 53.6 mAh g^{-1}) and no significant decay in capacity was noticed for up to 1000 cycles at a current density of 1 A g^{-1} (Fig. S13a, ESI†). TP showed higher capacity as a cathode material than as an anode material, which can be ascribed to the insertion of both Li^+ and PF_6^- ions in the cathode region, while only Li^+ cations were interacted in the anode region. Meanwhile, this result further confirms the bipolar feature of the TP molecule.

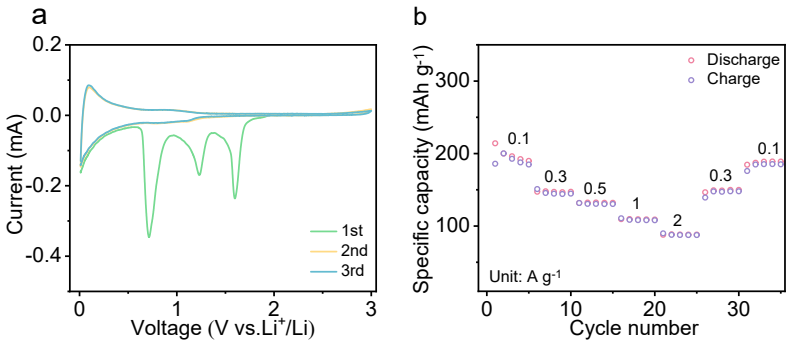

Fig. S12. a) The CV curve of TP anode at a scan rate 0.3 mv s^{-1}. b) Rate capability of TP anode.

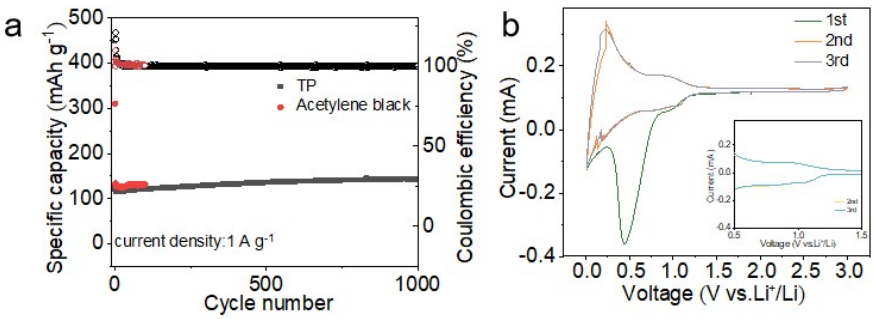

Fig. S13. (a) Cycling performance of the TP anode and acetylene black at 1 A g^{-1}. (b) The CV curve of acetylene balck at a scan rate 0.3 mv s^{-1}

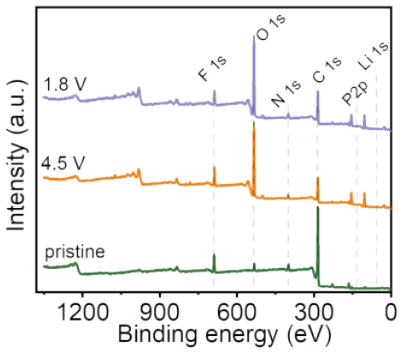

Fig. S14. The survey spectra of TP cathode at different charged states.

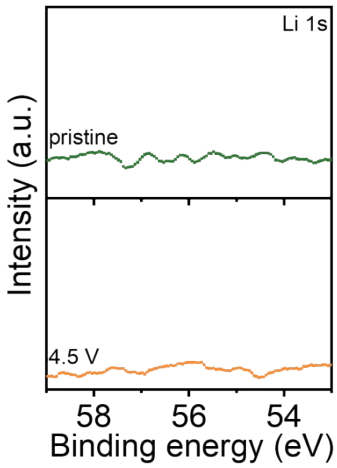

Fig. S15. The Li 1s XPS spectra of TP.

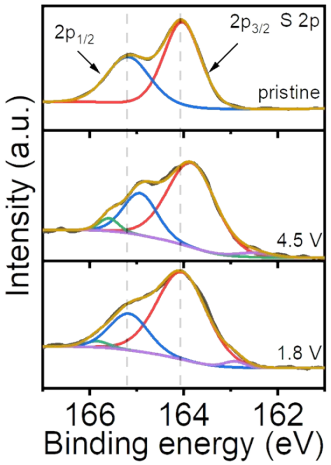

Fig. S16. The S 2p XPS spectra of TP.

When TP was used as the anode, the Li element was detected in the survey spectra of different voltage states (Fig. S17, ESI†), which suggests that Li^+ ions are inserted TP molecule. The LiF was monitored in the fully discharged state (Fig. S18, ESI†), implying the formation of a solid electrolyte interface (SEI). Compared to the pristine of N 1s, the peak intensity with binding energy at 400.1 eV of the C-N bond was increased, and the peak intensity of the C=N bond with binding energy at 397.8 eV was decreased during the discharge (Fig.S19, ESI†). This result suggests that Li^+ reacts reversibly with N atoms of porphyrin. Compared to the pristine of the S 2p core level XPS spectra, the peak shifted to 165.3 and 164.1 eV during the discharging process (Fig.S20, ESI†). This result indicates that the N atom and S atom act as active sites to accommodate lithium-ion.

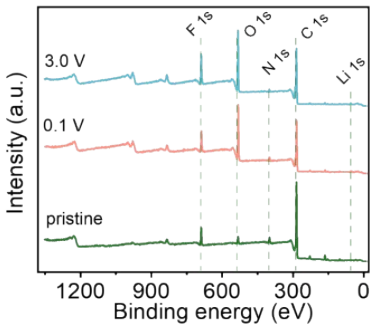

Fig. S17. The survey spectra of TP anode at different charged states.

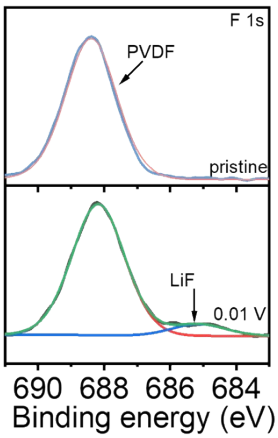

Fig. S18. The XPS spectra of F element.

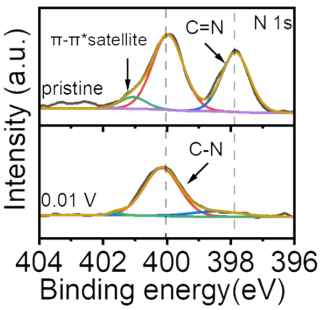

Fig. S19. The N 1s XPS spectra of TP.

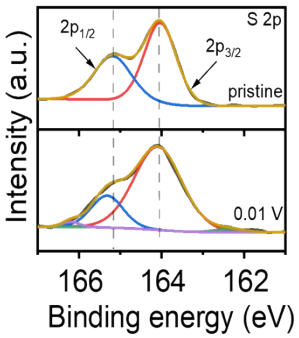

Fig. S20. The XPS spectra of S element.

4. Supplementary Tables

Table S1. Comparison of electrochemical performance of TP all-symmetric cells with reported systems for all-organic symmetrical cells.

Cathode/anode	**Working voltage (V)**	**Discharge voltage (V)**	**Reversible capacity (mA h g^{-1}, current density A g^{-1})**	**Capacity retention (Current density A g^{-1}, cycle number)**	**Ref.**
TP/TP	1.0-4.0	2.7	153 (0.2)	62% (1, 1500)	This work
PSQ/PSQ	1.0-4.0	1.4	170 (0.05)	48% (2, 3000)	1
LiTCNQ/Li_2TPh	1.3-2.4	1.8	150 (0.02)	70% (0.02, 50)	2
Ni-TABQ/Ni-TABQ	0.1-2.9	0.8	169 (0.05)	69% (0.2, 50)	3
Li_4TP/Na_2AQ26DS	0.2-3.3	1.1	120 (0.05)	52% (0.5, 1200)	4
CuPcNA-CMP/CuPcNA-CMP	1.0-4.0	2.5	198 (0.05)	68% (0.1, 200)	5
ABB4OLi/Li_4TP	1.0-3.0	1.0	120 (0.05)	52% (0.05, 200)	6
CuTAPc/ CuTAPc	1.0-4.0	2.1	110 (0.2)	54% (0.2, 200)	7
PZDV/PZDB	1.5-4.0	2.5	55 (0.123)	100% (0.12, 200)	8

Reference

1. J. Wang, H. C. Liu, C. Y. Du, Y. Liu, B. Liu, H. R. Guan, S. W. Guan, Z. H. Sun and H. Y. Yao, *Chem. Sci.*, 2022, 13, 11614- 11622.
2. W. W. Deng, W. B. Shi, P. Y. Li, N. Q. Hu, S. C. Wang, J. Y. Wang, L. Liu, Z. Z. Shi, J. Lin and C. X. Guo, *Energy Storage Mater.*, 2022, **46**, 535-541
3. K. Li, J. Yu, Z. J. Si, B. Gao, H. G. Wang and Y. H. Wang, *Chem. Eng. J.*, 2022, **450**, 138052.
4. W. Q. Liu, W. Tang, X. P. Zhang, Y. Hu, X. X. Wang, Y. C. Yan, L. Xu and C. Fan, *Int. J. Hydrogen Energy*, 2021, **46**, 36801-36810.
5. H. G. Wang, Q. Li, Q. Wu, Z. J. Si, X. L. Lv, X. T. Liang, H. L. Wang, L. Sun, W. D. Shi and S. Y. Song, *Adv. Energy Mater.*, 2021, **11**, 2100381.
6. Y. Hu, W. Tang, Q. H. Yu, C. L. Yang and C. Fan, *ACS Appl. Mater. Interfaces.*, 2019, **11**, 32987-32993.
7. H. G. Wang, H. Wang, Z. Si, Q. Li, Q. Wu, Q. Shao, L. Wu, Y. Liu, Y. Wang, S. Song and H. Zhang, *Angew. Chem. Int. Ed.*, 2019, **58**, 10204-10208.
8. G. L. Dai, Y. He, Z. H. Niu, P. He, C. K. Zhang, Y. Zhao, X. H. Zhang and H. S. Zhou, *Angew. Chem. Int. Ed.*, 2019, **58**, 9902-9906.